

# Improved High-Efficiency Organic Solar Cells via Incorporation of a Conjugated Polyelectrolyte Interlayer

Jung Hwa Seo,<sup>†</sup> Andrea Gutacker,<sup>‡</sup> Yanming Sun,<sup>†</sup> Hongbin Wu,<sup>§</sup> Fei Huang,<sup>§</sup> Yong Cao,<sup>§</sup> Ullrich Scherf,<sup>‡</sup> Alan J. Heeger,<sup>†</sup> and Guillermo C. Bazan<sup>\*,†</sup>

<sup>†</sup>Center for Polymers and Organic Solids, Department of Physics, and Department of Chemistry and Biochemistry, University of California, Santa Barbara, California 93106, United States

<sup>‡</sup>Makromolekulare Chemie, Bergische Universität Wuppertal, D-42097 Wuppertal, Germany

<sup>§</sup>Institute of Polymer Optoelectronic Materials and Devices, South China University of Technology, Guangzhou 510640, P. R. China

**S** Supporting Information

**ABSTRACT:** The power conversion efficiencies of bulk heterojunction (BHJ) solar cells can be increased from 5 to 6.5% by incorporating an ultrathin conjugated polyelectrolyte (CPE) layer between the active layer and the metal cathode. Poly[*N*-9'-heptadecanyl-2,7-carbazole-*alt*-5,5-(4',7'-di-2-thienyl-2',1',3'-benzothiadiazole)] (PCDTBT) and [6,6]-phenyl C<sub>71</sub> butyric acid methyl ester (PC<sub>71</sub>BM) were chosen for the photoactive layer. CPEs with cationic polythiophenes, in both homopolymer and block copolymer configurations, were used to improve the electronic characteristics. The significant improvement in device performance and the simplicity of fabrication by solution processing suggest a promising and practical pathway for improving polymer solar cells with high efficiencies.

Bulk heterojunction (BHJ) solar cells based on blends comprising conjugated polymers and fullerene acceptors are the subject of considerable investigation because of their potential to enable the fabrication of low-cost devices that convert sunlight into electricity.<sup>1</sup> Significant improvements in power conversion efficiencies (PCEs) due to combined improvements in materials design,<sup>2</sup> interface control,<sup>3</sup> self-assembly of donor and acceptor phases,<sup>4</sup> and device fabrication and engineering<sup>5</sup> have recently appeared.

The fundamental quantities that determine the PCE include the open-circuit voltage ( $V_{oc}$ ), the short-circuit current density ( $J_{sc}$ ), and the fill factor (FF), as shown in eq 1:

$$PCE = \frac{V_{oc} \cdot J_{sc} \cdot FF}{P_{in}} \quad (1)$$

where  $P_{in}$  is the power of the incident light. In BHJ solar cells,  $V_{oc}$  has been correlated with the energy difference between the highest occupied molecular orbital (HOMO) of the polymer (donor) and the lowest unoccupied molecular orbital (LUMO) of the fullerene (acceptor).<sup>1–5</sup> To minimize the contact resistance, the interface between the active layer and the electrodes should be ohmic.<sup>1b,d</sup> Such a requirement has led to efforts in interfacial engineering, including the use of thermally deposited LiF<sup>6</sup> or bathocuproine (BCP),<sup>7</sup> self-assembled monolayers (SAMs),<sup>8</sup> and metal oxides (i.e., TiO<sub>2</sub>, CsCO<sub>3</sub>, MoO<sub>3</sub>, and ZnO).<sup>9</sup>

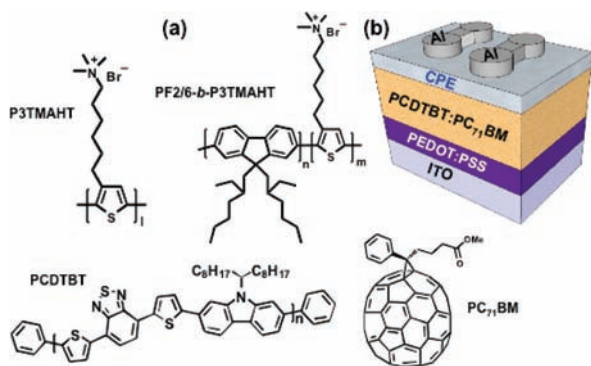
Conjugated polyelectrolytes (CPEs), which are conjugated polymers with pendant groups bearing ionic functionalities, are promising interfacial layer materials in organic electronic devices such as organic light-emitting devices,<sup>10</sup> thin-film transistors,<sup>11</sup> and solar cells<sup>12</sup> as well as biological and chemical sensors.<sup>13</sup> Their solubility in highly polar solvents allows the simple fabrication of multi-layer organic devices by avoiding the problem of disturbing neutral organic semiconducting layers that are typically miscible in aromatic solvents.<sup>14</sup> A combination of techniques, including UV photoelectron spectroscopy (UPS), has shown that CPE deposition can influence the work function of adjacent electrodes.<sup>15</sup> Recently, polyfluorene-based CPEs and related materials have been inserted between the active layer and the electron-collecting electrode in BHJ devices to achieve increases in  $V_{oc}$ . This approach has led to devices with PCEs in the 1–4% range.<sup>12a–c</sup> However, examination of refs 12b and 12c shows that there is a strong and poorly understood dependence of the  $V_{oc}$  increase on the chemical nature of the CPE and the donor polymer. Furthermore, none of these devices reached a PCE above 4%.

In this contribution, we demonstrate that the insertion of an ultrathin CPE layer from methanol solution beneath Al cathodes can be an effective strategy for increasing the PCE from ~5 to ~6.5%. We also show that simply treating the BHJ layer with methanol can have a substantial positive effect on device performance. Leclerc-type carbazole-based conjugated copolymers were chosen as the donor material in our studies. Scheme 1 shows the structures of all of the materials and the device test structure. To examine the CPE function, two cationic poly(thiophene) derivatives were used: the homopolymer poly[3-(6-trimethylammoniumhexyl)thiophene] (P3TMAHT) and the ionic conjugated diblock copolymer poly(9,9-bis(2-ethylhexyl)-fluorene)-*b*-poly[3-(6-trimethylammoniumhexyl)thiophene] (PF2/6-*b*-P3TMAHT).<sup>16</sup> It is interesting to note that a polythiophene framework would be anticipated to be more functional as a hole transport layer than to facilitate electron extraction.<sup>1b–e,2c</sup> Specifically, the polythiophene backbones of P3TMAHT and PF2/6-*b*-P3TMAHT would be estimated to be described by a HOMO energy on the order of 5 eV, which is close to the work function of poly(3,4-ethylenedioxythiophene):poly(styrenesulfonate) (PEDOT:PSS)<sup>9a</sup> and the HOMO level (5.5 eV) of poly[*N*-9'-heptadecanyl-2,7-carbazole-*alt*-5,5-(4',7'-di-2-thienyl-2',1',3'-benzothiadiazole)]

Received: February 13, 2011

Published: May 10, 2011

Scheme 1. (a) Molecular Structures of the Materials Used for Device Fabrication;<sup>a</sup> (b) Device Configuration for the Solar Cells Used in This Study



<sup>a</sup> In PF2/6-*b*-P3TMAHT, the average values of *n* and *m* were 16 and 27, respectively.

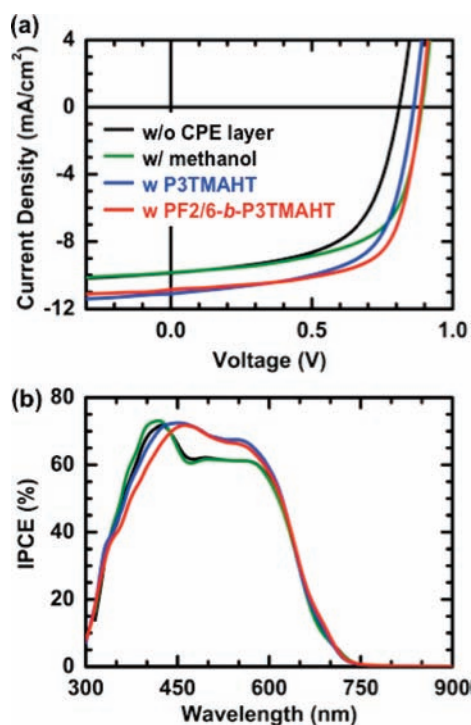


**Figure 1.** (a)  $J$ - $V$  characteristics of PCDTBT:PC<sub>71</sub>BM devices with no CPE layer (black) and thin layers of P3TMAHT (blue) and PF2/6-*b*-P3TMAHT (red) under illumination of an AM 1.5G solar simulator (100 mW/cm<sup>2</sup>). Methanol (green) was spin-cast on top of the active layer for comparison. (b) IPCE spectra of BHJ solar cells corresponding to (a).

(PCDTBT).<sup>2a,9a</sup> However, as will be described below, the two CPEs can substantially improve the solar cell efficiency when they are placed adjacent to an electron-collecting Al electrode.

Detailed methods for the syntheses of P3TMAHT and PF2/6-*b*-P3TMAHT are described in the literature.<sup>16</sup> Devices were fabricated by spin-casting the BHJ blend from a 1:3 chlorobenzene/1,2-dichlorobenzene solvent mixture atop a 40 nm thick PEDOT:PSS layer on glass substrates patterned with indium tin oxide (ITO). PCDTBT and [6,6]-phenyl C<sub>71</sub> butyric acid

**Table 1.** Device Performance of PCDTBT:PC<sub>71</sub>BM BHJ Solar Cells with and without CPE Layers

PCDTBT:PC <sub>71</sub> BM	$J_{sc}$ (mA/cm <sup>2</sup> )	$V_{oc}$ (V)	FF (%)	PCE (%)	
				avg	best
without CPE layer	9.7 ± 0.3	0.82 ± 0.04	61 ± 2	5.0	5.3
with methanol	9.7 ± 0.3	0.88 ± 0.01	62 ± 1	5.3	5.4
with P3TMAHT	10.8 ± 0.3	0.86 ± 0.01	66 ± 1	6.1	6.3
with PF2/6- <i>b</i> -P3TMAHT	10.6 ± 0.3	0.89 ± 0.01	67 ± 1	6.2	6.5

methyl ester (PC<sub>71</sub>BM) were selected as the BHJ components.<sup>9a</sup> The CPE layers were subsequently deposited by spin-casting from 0.01% (w/v) P3TMAHT and 0.02% (w/v) PF2/6-*b*-P3TMAHT solutions in methanol. These low concentrations were chosen to minimize thicknesses and prevent possible complications due to ion motion and concomitant redistribution of internal electric fields in the device.<sup>11</sup>

Current density–voltage ( $J$ - $V$ ) characteristics of the devices measured under AM 1.5G irradiation are shown in Figure 1a. The resulting  $J_{sc}$ ,  $V_{oc}$ , FF, and PCE values, as determined from the  $J$ - $V$  curves, are summarized in Table 1. Relative to the initial control device, the introduction of the CPE layer led to increases in  $J_{sc}$  from 9.7 mA/cm<sup>2</sup> to 10.8 mA/cm<sup>2</sup> (P3TMAHT) and 10.6 mA/cm<sup>2</sup> (PF2/6-*b*-P3TMAHT). Similarly,  $V_{oc}$  improved from 0.82 V to 0.86 V (P3TMAHT) and 0.89 V (PF2/6-*b*-P3TMAHT) and FF from 63% to 66% (P3TMAHT) and 67% (PF2/6-*b*-P3TMAHT). Thus, on the basis of eq 1, the PCE increased from 5.3% for the control device to 6.3% (P3TMAHT) and 6.5% (PF2/6-*b*-P3TMAHT).

A second type of control device was also fabricated to probe possible influences by the deposition and subsequent removal of the methanol solvent. These experiments involved deposition of methanol atop the active layer followed by a sequence of steps similar to those for the CPE devices described above. As shown by the green trace in Figure 1 and the data in Table 1, the methanol-treated devices showed increased  $V_{oc}$  values and higher PCEs. However, the  $J_{sc}$  values were not as high as for the CPE-treated devices. We surmise at this point that the improvement in performance after CPE deposition may be due to a combination of the effects of methanol treatment and the presence of the thin CPE layer.

The  $J$ - $V$  characteristics of the devices obtained under dark conditions are given in the Supporting Information. In the regime from -1 to 0.8 V, the dark current densities with the CPE layers were significantly suppressed, consistent with reduced leakage current and increased shunt resistance ( $R_{sh}$ ) (0.5, 0.9, and 1.0 MΩ·cm<sup>2</sup> for the control, P3TMAHT, and PF2/6-*b*-P3TMAHT, respectively). For  $V > 0.8$  V, the series resistance ( $R_s$ ) of the control device was 3.5 Ω·cm<sup>2</sup>, and those for the devices with P3TMAHT and PF2/6-*b*-P3TMAHT were 3.0 and 2.6 Ω·cm<sup>2</sup>, respectively. Thus, the performance of devices incorporating CPE layers can be enhanced, since a good solar cell requires high  $R_{sh}$  and low  $R_s$ . The improved PCEs of the devices with CPE layers are also consistent with the higher incident photon-to-current efficiency (IPCE) values, which reached >70% (Figure 1b). It is worth pointing out that the performance of the PCDTBT:PC<sub>71</sub>BM devices incorporating the CPE layers was comparable to the highest values reported to date for these devices with a TiO<sub>x</sub> interlayer.<sup>9a,b</sup> CPE deposition, however, is simpler, since formation of a TiO<sub>x</sub> layer requires spin-casting of a precursor solution followed by thermal annealing.<sup>17</sup>

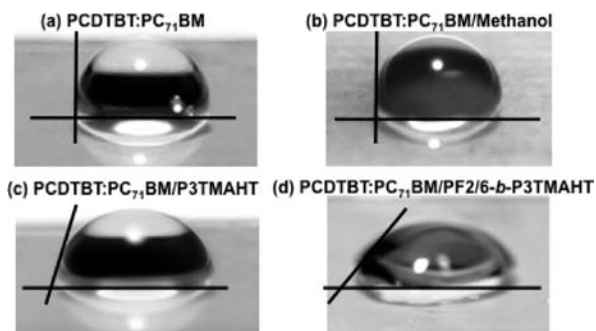


**Figure 2.** Photos of water droplets on the surfaces of (a) PCDTBT:PC<sub>71</sub>BM, (b) PCDTBT:PC<sub>71</sub>BM after spin-casting of methanol, (c) 0.01% P3TMAHT, and (d) 0.02% PF2/6-*b*-P3TMAHT on PCDTBT:PC<sub>71</sub>BM substrates.

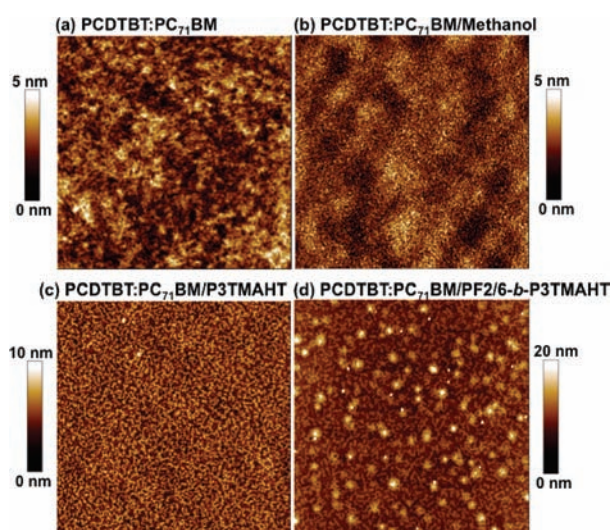


**Figure 3.** Surface topographic AFM images (size: 5 μm × 5 μm) of (a) the control PCDTBT:PC<sub>71</sub>BM layer, (b) the PCDTBT:PC<sub>71</sub>BM layer after treatment with methanol, (c) after deposition of P3TMAHT on the PCDTBT:PC<sub>71</sub>BM layer, and (d) after deposition of PF2/6-*b*-P3TMAHT on the PCDTBT/PC<sub>71</sub>BM layer.

Measurements of the water contact angle ( $\theta$ ) were performed on the surface of PCDTBT:PC<sub>71</sub>BM and PCDTBT:PC<sub>71</sub>BM/CPE layers as a function of treatment history, and the images were collected with a digital camera. As shown in Figure 2a, the PCDTBT:PC<sub>71</sub>BM surface ( $\theta \approx 90^\circ$ ) was largely hydrophobic and remained so upon treatment with neat methanol (Figure 2b). In contrast, the surfaces were moderately hydrophilic for P3TMAHT ( $\theta \approx 45^\circ$ ) and hydrophilic for PF2/6-*b*-P3TMAHT ( $\theta < 30^\circ$ ), which suggests accumulation of the ionic component at the topmost organic surface, as previously observed with other CPE multilayer structures.<sup>18</sup> These data are consistent with the block copolymer providing a more polar surface despite the presence of the hydrophobic polyfluorene segment. Our thinking is that the difference in polymer architecture leads to different organization atop the BHJ surface. However, knowledge of the exact orientation and accumulation of the ionic component on the surface requires further structural characterization studies.

Figure 3 shows the surface morphologies obtained by atomic force microscopy (AFM), as measured under an inert nitrogen atmosphere. The surface of PCDTBT:PC<sub>71</sub>BM was relatively

smooth, with a root-mean-square (rms) roughness of 0.41 nm (Figure 3a). The methanol-treated surface was slightly smoother (rms roughness = 0.25 nm) and remained homogeneous, as shown in Figure 3b. No obvious surface reconstruction was therefore apparent. In the case of the PCDTBT:PC<sub>71</sub>BM/P3TMAHT layer, connected features with average heights of 3 nm were observed (Figure 3c).<sup>19</sup> The PCDTBT:PC<sub>71</sub>BM/PF2/6-*b*-P3TMAHT layer featured raised islands connected by a thin network of terraces (Figure 3d). Deposition of the CPE layers under the experimental conditions described here thus resulted in increased roughness from  $\sim 0.41$  to  $\sim 2$  nm in the case of PCDTBT:PC<sub>71</sub>BM/PF2/6-*b*-P3TMAHT. Additionally, Kelvin probe force microscopy measurements showed that both CPE layers increased the average surface potential (see the Supporting Information). These observations are in agreement with the idea of local dipole arrangements that modify the contacts with the Al electrode.

In conclusion, we have demonstrated that it is possible to incorporate CPE layers to improve plastic solar cells with very good efficiencies, from 5 to >6%. Moreover, these CPEs are located adjacent to the electron-collecting electrode and are based on polythiophene backbones, which are typically considered hole transport materials. Block copolymers bearing CPE segments have also been shown to be useful, and despite the presence of a hydrophobic (polyfluorene) segment, one obtains hydrophilic and, by inference, polar surfaces. It is reasonable that this increased polarity relates to the accumulation of ions and the formation of an interfacial dipole layer. It has also been identified that methanol treatment can have a positive beneficial effect in the absence of CPE, particularly on  $V_{oc}$ . This change takes place without modification of topography or the apparent polarity of the active layer. At this point, we lack insight into possible swelling and redistribution of BHJ components at the interface. The important conclusion is that the simple deposition of the CPE layer introduces more than one phenomenon, which with this particular set of materials work in concert to increase  $V_{oc}$  and  $J_{sc}$ . These observations need to be considered to better understand the previous lack of consistency in the literature concerning the impact of CPE interlayers for managing solar cell performance. Despite these uncertainties, we note that the improvement obtained with CPEs is similar to that observed with TiO<sub>x</sub> interlayers, but the device fabrication is considerably simpler and amenable to solution deposition methods and does not require thermal annealing.

## ■ ASSOCIATED CONTENT

**S Supporting Information.** Experimental details, UV–vis absorption and UPS spectra, and AFM images and surface potential profiles. This material is available free of charge via the Internet at <http://pubs.acs.org>.

## ■ AUTHOR INFORMATION

**Corresponding Author**  
bazan@chem.ucsb.edu

## ■ ACKNOWLEDGMENT

The authors are grateful to the NSF (DMR 0606414) for financial support. This research was also partially supported by the U.S. Army General Technical Services (LLC/GTS-S-09-1-196)

and the Department of Energy (DOE ER46535). We thank Dr. D. Waller (Konarka Technologies) for providing the PCDTBT and PC<sub>71</sub>BM materials.

## REFERENCES

- (1) (a) Yu, G.; Gao, J.; Hemmelen, J. C.; Wudl, F.; Heeger, A. J. *Science* **1995**, *270*, 1789. (b) Gunes, S.; Neugebauer, H.; Sariciftci, N. S. *Chem. Rev.* **2007**, *107*, 1324. (c) Blom, P. W. M.; Mihaileti, V. D.; Koster, L. J. A.; Markov, D. E. *Adv. Mater.* **2007**, *19*, 1551. (d) Dennler, G.; Scharber, M. C.; Brabec, C. J. *Adv. Mater.* **2009**, *21*, 1323. (e) Chen, L. M.; Xu, Z.; Hong, Z.; Yang, Y. *J. Mater. Chem.* **2010**, *20*, 2575.
- (2) (a) Blouin, N.; Michaud, A.; Gendron, D.; Wakim, S.; Blair, E.; Neagu-Plesu, R.; Belletête, M.; Durocher, G.; Tao, Y.; Leclerc, M. *J. Am. Chem. Soc.* **2008**, *130*, 732. (b) Kim, B.; Miyamoto, Y.; Ma, B.; Fréchet, J. M. J. *Adv. Funct. Mater.* **2009**, *19*, 2273. (c) Chen, H.-Y.; Hou, J.; Zhang, S.; Liang, Y.; Yang, G.; Yang, Y.; Yu, L.; Wu, Y.; Li, G. *Nat. Photonics* **2009**, *3*, 649.
- (3) (a) Sharma, G. D.; Suresh, P.; Sharma, S. S.; Vijay, Y. K.; Mikroyannidis, J. A. *ACS Appl. Mater. Interfaces* **2010**, *2*, 504. (b) Kim, Y.; Choulis, S. A.; Nelson, J.; Bradley, D. D. C.; Cook, S.; Durrant, J. R. *J. Mater. Sci.* **2004**, *40*, 1371. (c) Mayer, A. C.; Scully, S. R.; Hardin, B. E.; Rowell, M. W.; McGehee, M. D. *Mater. Today* **2007**, *10*, 28. (d) Stein, R.; Kogler, F. R.; Brabec, C. J. *J. Mater. Chem.* **2010**, *20*, 2499.
- (4) (a) Brabec, C. J.; Padinger, F.; Hummelen, J. C.; Janssen, R. A. J.; Sariciftci, N. S. *Synth. Met.* **1999**, *102*, 861. (b) Peet, J.; Kim, J. Y.; Coates, N. E.; Ma, W. L.; Moses, D.; Heeger, A. J.; Bazan, G. C. *Nat. Mater.* **2007**, *6*, 497. (c) Coffrey, D. C.; Reid, O. G.; Rodovsky, D. B.; Bartholomew, G. P.; Ginger, D. S. *Nano Lett.* **2007**, *7*, 738.
- (5) (a) Jo, J.; Kim, S.-S.; Na, S.-I.; Yu, B.-K.; Kim, D.-Y. *Adv. Funct. Mater.* **2009**, *19*, 866. (b) Al-Ibrahim, M.; Ambacher, O.; Sensfuss, S.; Gobsch, G. *Appl. Phys. Lett.* **2005**, *86*, No. 201120. (c) Li, G.; Chu, C.-W.; Shrotriya, V.; Huang, J.; Yang, Y. *Appl. Phys. Lett.* **2006**, *88*, No. 253503.
- (6) (a) Brabec, C. J.; Shaheen, S. E.; Winder, C.; Sariciftci, N. S.; Denk, P. *Appl. Phys. Lett.* **2002**, *80*, 1288. (b) Yang, X.; Loos, J.; Veenstra, S. C.; Verhees, W. J. H.; Wienk, M. M.; Kroon, J. M.; Michels, M. A. J.; Janssen, R. A. J. *Nano Lett.* **2005**, *5*, 579.
- (7) (a) Peumans, P.; Yakimov, A.; Forrest, S. R. *J. Appl. Phys.* **2003**, *93*, 3693. (b) Chang, C.-C.; Lin, C.-F.; Chiou, J.-M.; Ho, T.-H.; Tai, Y.; Lee, J.-H.; Chen, Y.-F.; Wang, J.-K.; Chen, L.-C.; Chen, K.-H. *Appl. Phys. Lett.* **2010**, *96*, No. 263506.
- (8) Yip, H.-L.; Hau, S. K.; Baek, N. S.; Ma, H.; Jen, A. K.-J. *Adv. Mater.* **2008**, *20*, 2376.
- (9) (a) Park, S. H.; Roy, A.; Beaupré, S.; Cho, S.; Coates, N.; Moon, J. S.; Moses, D.; Leclerc, M.; Lee, K.; Heeger, A. J. *Nat. Photonics* **2009**, *3*, 297. (b) Lee, J. H.; Cho, S.; Roy, A.; Jung, H.-T.; Heeger, A. J. *Appl. Phys. Lett.* **2010**, *96*, No. 163303. (c) Li, G.; Chu, C. W.; Shrotriya, V.; Huang, J.; Yang, Y. *Appl. Phys. Lett.* **2006**, *88*, No. 253503. (d) Zhao, D. W.; Liu, P.; Sun, X. W.; Tan, S. T.; Ke, L.; Kyaw, A. K. K. *Appl. Phys. Lett.* **2009**, *95*, No. 153304. (e) White, M. S.; Olson, D. C.; Shaheen, S. E.; Kopidakis, N.; Ginley, D. S. *Appl. Phys. Lett.* **2006**, *89*, No. 143517.
- (10) (a) Hoven, C. V.; Yang, R.; Garcia, A.; Crockett, V.; Heeger, A. J.; Bazan, G. C. *Proc. Natl. Acad. Sci. U.S.A.* **2008**, *105*, 12730. (b) Bolink, H. J.; Brine, H.; Coronado, E.; Sessolo, M. *ACS Appl. Mater. Interfaces* **2010**, *2*, 2694.
- (11) (a) Seo, J. H.; Gutacker, A.; Walker, B.; Cho, S.; Garcia, A.; Yang, R.; Nguyen, T.-Q.; Heeger, A. J.; Bazan, G. C. *J. Am. Chem. Soc.* **2009**, *131*, 18220. (b) Seo, J. H.; Namdas, E. B.; Gutacker, A.; Heeger, A. J.; Bazan, G. C. *Appl. Phys. Lett.* **2010**, *97*, No. 043303.
- (12) (a) Luo, J.; Wu, H.; He, C.; Li, A.; Yang, W.; Cao, Y. *Appl. Phys. Lett.* **2009**, *95*, No. 043301. (b) He, C.; Zhong, C.; Wu, H.; Yang, R.; Yang, W.; Huang, F.; Bazan, G. C.; Cao, Y. *J. Mater. Chem.* **2010**, *20*, 2617. (c) Oh, S.-H.; Na, S.-I.; Jo, J.; Lim, B.; Vak, D.; Kim, D.-Y. *Adv. Funct. Mater.* **2010**, *20*, 1997.
- (13) Wang, Y.; Liu, B.; Mikhailovsky, A.; Bazan, G. C. *Adv. Mater.* **2010**, *22*, 656.
- (14) (a) Hoven, C. V.; Garcia, A.; Bazan, G. C.; Nguyen, T.-Q. *Adv. Mater.* **2008**, *20*, 3793. (b) Huang, F.; Wu, B.; Cao, Y. *Chem. Soc. Rev.* **2010**, *39*, 2500. (c) Wang, C.; Garcia, A.; Yan, H.; Sohn, K. E.; Hexemer, A.; Nguyen, T.-Q.; Bazan, G. C.; Kramer, E. J.; Ade, H. *J. Am. Chem. Soc.* **2009**, *131*, 12538.
- (15) Seo, J. H.; Nguyen, T.-Q. *J. Am. Chem. Soc.* **2008**, *130*, 10042.
- (16) (a) Scherf, U.; Gutacker, A.; Koenen, N. *Acc. Chem. Res.* **2008**, *41*, 1086. (b) Scherf, U.; Adamczyk, S.; Gutacker, A.; Koenen, N. *Macromol. Rapid Commun.* **2009**, *30*, 1059. (c) Gutacker, A.; Adamczyk, S.; Helfer, A.; Garner, L. E.; Evans, R. C.; Fonseca, S. M.; Knaapila, M.; Bazan, G. C.; Burrows, H. D.; Scherf, U. *J. Mater. Chem.* **2010**, *20*, 1423. (d) Knaapila, M.; Evans, R. C.; Garamus, V. M.; Almásy, L.; Székely, N. K.; Gutacker, A.; Scherf, U.; Burrows, H. D. *Langmuir* **2010**, *26*, 15634. (e) Tu, G.; Li, H.; Forster, M.; Heiderhoff, R.; Balk, L. J.; Sigel, R.; Scherf, U. *Small* **2007**, *3*, 1001.
- (17) Kim, J. Y.; Kim, S. H.; Lee, H. H.; Lee, K.; Ma, W. L.; Gong, X.; Heeger, A. J. *Adv. Mater.* **2006**, *18*, 572.
- (18) Park, J.; Yang, R.; Hoven, C. V.; Garcia, A.; Fischer, D. A.; Nguyen, T.-Q.; Bazan, G. C.; DeLongchamp, D. M. *Adv. Mater.* **2008**, *20*, 2491.
- (19) Chen, Z.; Dang, X.-D.; Gutacker, A.; Garcia, A.; Li, H.; Xu, Y.; Ying, L.; Nguyen, T.-Q.; Bazan, G. C. *J. Am. Chem. Soc.* **2010**, *132*, 12160.